Journal of Materials Chemistry B

Accepted Manuscript

ROYAL SOCIETY OF CHEMISTRY

www.rsc.org/materialsB

Journal Name

COMMUNICATION

Gemcitabine and Chlorotoxin Conjugated Iron Oxide Nanoparticles for Glioblastoma Therapy

Qingxin Mu,[a, d] Guanyou Lin,[b] Victoria K. Patton,[c] Kui Wang,[a] Oliver W. Press,[d] Miqin Zhang[a]*

parReceived 00th January 20xx,
Accepted 00th January 20xx

DOI: 10.1039/x0xx00000x

www.rsc.org/

Many small-molecule anti-cancer drugs have short blood half-lives and toxicity issues due to non-specificity. Nanotechnology has shown great promise in addressing these issues. Here, we report the development of an anti-cancer drug gemcitabine-conjugated iron oxide nanoparticle for glioblastoma therapy. A glioblastoma targeting peptide, chlorotoxin, was attached after drug conjugation. The nanoparticle has a small size (~32 nm) and uniform size distribution (PDI ≈ 0.1), and is stable in biological medium. The nanoparticle effectively enter cancer cells without losing potency compared to free drug. Significantly, the nanoparticle showed a prolonged blood half-life and the ability to cross the blood-brain barrier in wild type mice.

Many small molecule anti-cancer drugs encounter short blood half-life and off-target toxicity issues.[1, 2] Alternatively, drugs can be formulated into nanoparticles (NPs) to improve their overall pharmacokinetic profiles.[3] One such an example is gemcitabine (GEM). GEM is an FDA-approved anti-cancer drug for treatments of pancreatic cancer, non-small cell lung cancer, breast cancer, ovarian cancer, bladder cancer, etc.[4-9] GEM has also been tested for brain tumour therapy.[10, 11] The activity of GEM in brain tumour therapy is independent of methylguanine methyltransferase (MGMT) expression, an enzyme that is responsible for resistance to temozolomide (TMZ), first-line brain tumour treatment drug.[12] However, GEM has a half-life of ~0.28 h in human and mice and several side effects.[4, 13] To address these issues, GEM has been modified and formulated into NPs. For example, GEM has been chemically modified with lipids (squalenoyl, stearoyl, etc.) to form lipid nanoparticles or loaded into liposomes to prolong blood circulation.[14-17] GEM has been loaded onto polymeric NPs such as chitosan and polybutylcyanoacrylate NPs for targeted drug delivery.[18, 19] However, these NPs were either too large (>100 nm) to pass BBB or colloidally unstable in biological medium for brain tumour therapy.

Here, we report the development of a small and colloidally stable GEM-loaded nanocarrier to increase GEM's circulation time and overcome blood-brain barrier (BBB) for targeted glioblastoma multiform (GBM) therapy. The nanocarrier is made of iron oxide-based NP immobilized with GEM, chlorotoxin (CTX), and hyaluronic acid (HA). GBM is the most common and aggressive malignant primary brain tumour with very poor prognosis.[20] Unlike liposomes or polymeric NPs, iron oxide NPs (IONPs) are small, stable and have superparamagnetic properties.[21-23] IONPs are also biodegradable and sterilizable, making them a suitable candidate for an effective drug delivery carrier.[21, 24] CTX is a 39-mer peptide that is able to cross the BBB and target brain tumour cells.[25] We have previously demonstrated brain tumour targeting of CTX-conjugated NPs.[23, 26, 27] Tumour targeting ligands could be used to deliver drugs specifically to tumors and reduce systemic toxicity.[28] A biodegradable cross linker, hyaluronic acid (HA), was used to bridge GEM and CTX with IONPs. HA is an anionic, non-sulfated glycosaminoglycan that naturally presents in human tissues. HA possesses repeated carboxyl groups on its glucuronic acid units that facilitates various chemical modifications and increase drug loading.[29] A low molecular weight HA of ~5 kDa was used in this study. The GEM and CTX conjugated IONPs (IONP-HA-GEM-CTX) (Scheme 1) were physicochemically characterized regarding physical and hydrodynamic sizes, ζ-potential, drug loading and medium stability. The cellular uptake of NPs and their effect on the potency in cell killing were evaluated. Furthermore, pharmacokinetics, biodistribution, and BBB penetration of IONP-HA-GEM-CTX in wild type mice, were also studied.

[a] Department of Materials Science and Engineering, University of Washington, Seattle, Washington, 98195, USA.
[b] Department of Bioengineering, University of Washington, Seattle, Washington, 98195, USA.
[c] Department of Chemical Engineering, University of Washington, Seattle, Washington, 98195, USA.
[d] Clinical Research Division, Fred Hutchinson Cancer Research Centre, Seattle, Washington, 98109, USA.
† Email: mzhang@uw.edu.
Electronic Supplementary Information (ESI) available: [details of any supplementary information available should be included here]. See DOI: 10.1039/x0xx00000x

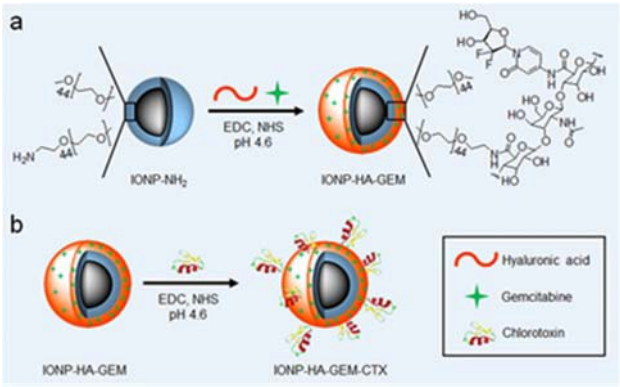

Scheme 1. Preparation of IONP-HA-GEM-CTX. a. conjugation of GEM onto IONP-NH_2. b. conjugation of CTX onto IONP-HA-GEM.

The IONP-HA-GEM-CTX was synthesized by firstly conjugating GEM onto IONPs using HA as a bridging molecule (Scheme 1a) followed by conjugation of CTX (Scheme 1b). 1-Ethyl-3-(3-dimethylaminopropyl)carbodiimide) EDC and N-Hydroxysuccinimide (NHS) were used for coupling of carboxyl and amine groups in these steps. CTX was conjugated onto carboxyl groups of HA, which was conjugated onto IONPs in first step. According to the synthesis procedure of IONP-PEG-NH_2, some PEG coatings on IONP had amine groups (Scheme 1a and Supplementary Information). IONP-HA-GEM-CTX was examined with transmission electron microscopy (TEM) with negative staining by uranyl acetate. The TEM images showed that these NPs had a core size of ~12.5 nm with uniform spherical shape (Figure 1a). With negative staining, we were able to visualize surface coating of NPs. The bright circles around IONPs indicated that the IONPs had a surface coating with thickness of ~2.5 nm. However, when dispersed in aqueous solutions, NPs had a hydrodynamic size of ~32 nm (Figure 1b, d) and a very narrow size distribution (PDI ≈ 0.1). The NPs with and without CTX conjugation had slightly different ζ-potential while both were near neural (Figure 1c, d). As GEM has a primary amine and may interact with HA electrostatically during conjugation process, we tested the drug loading with and without EDC and (NHS) presence. GEM was extracted from NPs after conjugation and analysed by high-performance liquid chromatography (HPLC). It was observed that, with EDC and NHS, a clear and sharp GEM peak was observed. However, without EDC and NHS, no GEM could be detected indicating no physical absorption onto NPs (Figure 1e). The number of GEM per NPs was determined to be ~20 (based on ~0.64 nmol NP per mg Fe). The number of CTX per particle on IONP-HA-GEM-CTX was estimated to be 5 ± 1.4 (based on free CTX after conjugation). The stability of NPs in cell culture medium was also tested. IONP-HA-CTX and IONP-HA-GEM-CTX were incubated with complete DMEM supplemented with 10% FBS and antibiotics at 37 °C. The hydrodynamic sizes were monitored over a two-week period. The size of NPs only increased slightly (Figure 1f), likely due to serum protein absorption.[30] This indicates that the NPs had excellent stability in biological media which contain plenty of ions, proteins, amino acids, etc.

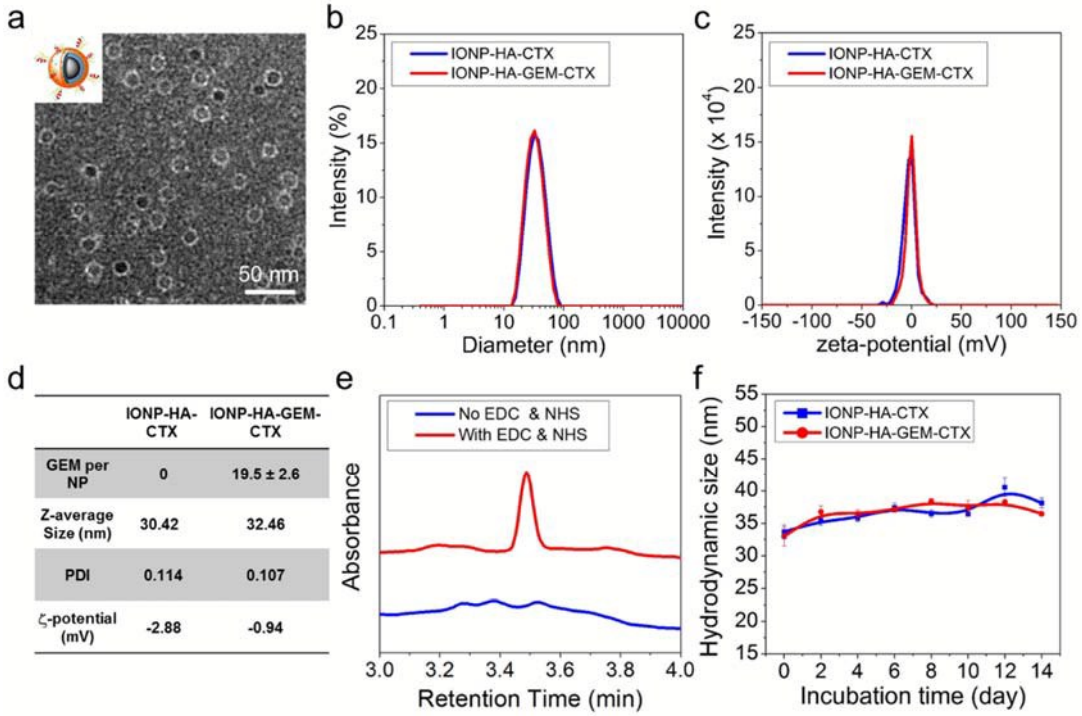

Figure 1. Characterization of NPs. a. TEM micrograph of IONP-HA-GEM-CTX. Inset: cartoon illustration of a coated IONP. b and c. Size distribution of IONP-HA-GEM and IONP-HA-GEM-CTX weighed by intensity (b) and their ζ-potentials at pH 7.4 (c) as measured with DLS. d. Properties of IONP-HA-CTX and IONP-HA-GEM-CTX. e, HPLC analysis of GEM extracted from IONP-HA-GEM synthesized with or without presence of EDC and NHS. f, Stability of IONP-HA-CTX and IONP-HA-GEM-CTX in complete DMEM cell culture medium at 37°C as determined by hydrodynamic size monitoring over 14 days.

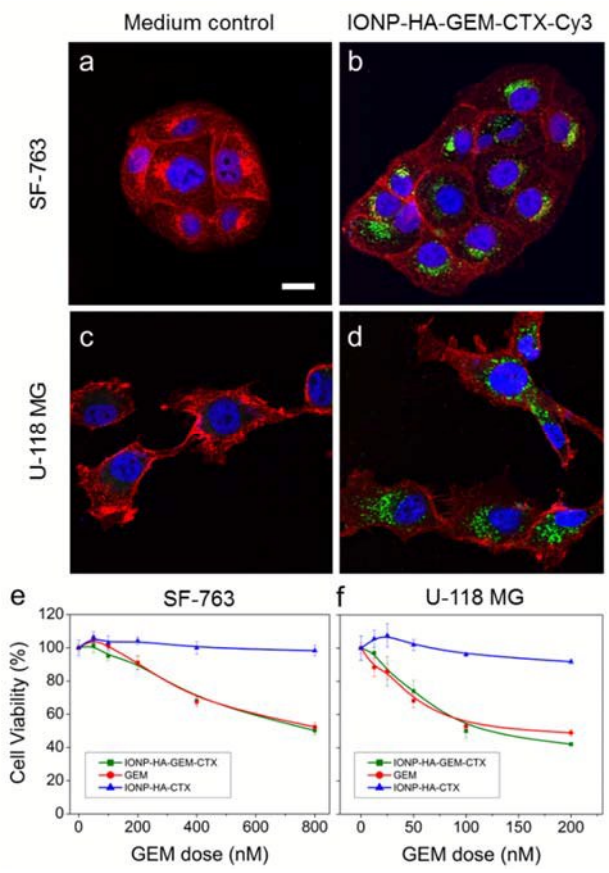

Figure 2. Cellular uptake of IONP-HA-GEM-CTX-Cy5.5 and viability after different treatments. a and c, SF-763 (a) and U-118 MG (c) with medium control; b and d, SF-763 (b) and U-118 MG (d) incubated with IONP-HA-GEM-CTX-Cy5.5 (40 μg/mL [Fe]) for 2 h. Blue, cell nucleus; red, cell membrane (false-coloured); green, NPs (false-coloured); e and f, cell viability of SF-763 (e) and U-118 MG (f) after treatments of IONP-HA-GEM-CTX, IONP-HA-CTX or free GEM for 72 h.

To study the cellular uptake of NPs, IONP-HA-GEM-CTX was labeled with Cy3 for visulization in cells. HA was first reacted with Cy3-hydrazide through carboxyl-hydrazide reaction before conjugation onto IONPs. Two human GBM cell lines, SF-763 and U-118 MG, were used, representing different expressions of MGMT, which is responsible for the degree of TMZ resistance.[31, 32] The cells were incubated with NPs for 2 h, washed, fixed and stained with nucleus and membrane dyes. Cells were then mounted onto glass slides and imaged with a Leica SP8 confocal microscope. For easy visulization, cell membranes and NPs were colored with red and green, respectively. It was shown that IONP-HA-GEM-CTX-Cy3 entered cells effectively and distributed in the cytoplasm around nuclei (Figure 2b, d).

The cell viability was then tested by the Alamar Blue assay. Cells were treated with GEM, IONP-HA-GEM-CTX or drug-free IONP-HA-CTX for 3 days. The results showed that IONP-HA-CTX had no effect on cell viability. GEM and IONP-HA-GEM-CTX showed a similar cell kill profile to both cell lines (Figure 2e, f). This suggests that after conjugating onto IONPs, GEM did not lose its potency as compared to free drug. The ultimate benefit of IONP-HA-GEM-CTX could be expected in vivo as a biodistribution of a drug played an important role on determining in vivo efficacy[33].

GEM has a short blood half-life (~0.28 h).[4, 13] As we have previously demonstrated long-lasting blood circulation with O^6-benzylguanine conjugated IONPs,[23] we expected that GEM-conjugated IONPs would show prolonged blood circulation as well. To verify this, we labelled the IONP-HA-GEM-CTX with a near infrared dye Cy5.5 similar to the aforementioned Cy3 labelling for *in vivo* detection purpose. The resultant IONP-HA-GEM-CTX-Cy5.5 was injected into wild type mice intravenously with 0.2 mg Fe equivalence per mouse. Blood samples were collected at various time points and the NP fluorescence from the blood sample was measured by a microplate reader (Ex: 673 nm; Em: 727 nm). At the meantime, various organs were collected at 3 and 48 h after NP injection for biodistribution study. Note that the mice behave normal throughout this experiment and 4 weeks after experiment, and there was no body weight loss, indicating non-toxicity of IONPs. From the pharmacokinetic profile of IONP-HA-GEM-CTX-Cy5.5, it can be seen that the clearance of NPs from blood circulation fits into a power law distribution curve (Figure 3a). The blood half-life was estimated to be ~2.8 h, which is 10 folds longer than free GEM.[13]

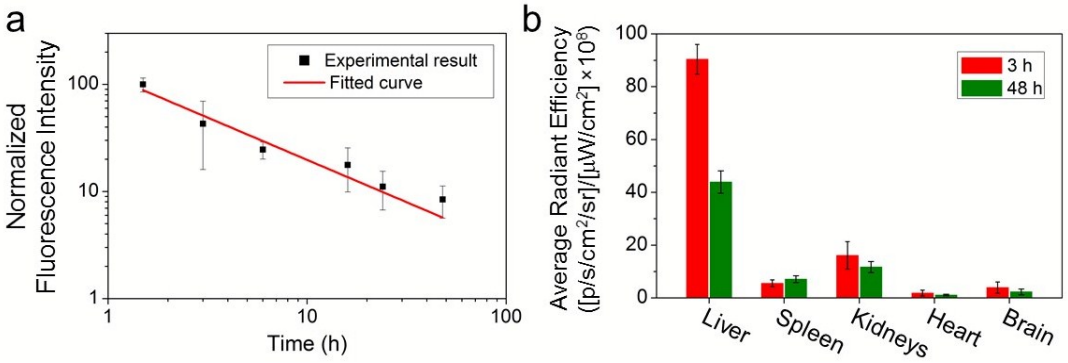

Figure 3. Pharmacokinetics and biodistribution of IONP-HA-GEM-CTX-Cy5.5 in wild type mice. a. Blood clearance profile of IONP-HA-GEM-CTX-Cy5.5 determined using fluorescence measurements. The curve indicates a power law distribution fit to the data (n = 3 mice per time point); b. *Ex vivo* measurement of fluorescence intensity from various organs 3 and 48 h post injection using the IVIS 200 imaging system.

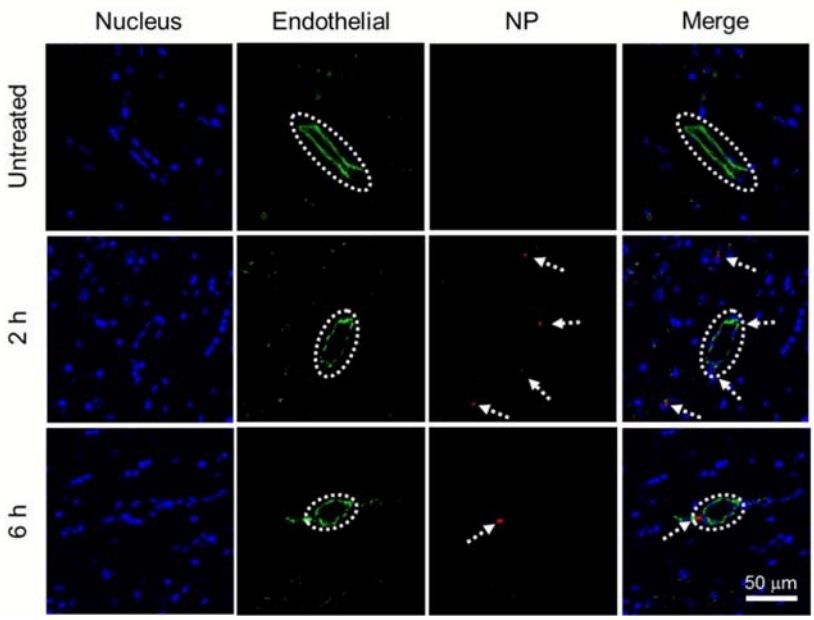

Figure 4. *In vivo* BBB permeability study. Confocal fluorescence microscopy images of mouse brain tissue sections with one of three treatment conditions: untreated (top), 2 h (middle) and 6 h (bottom) after injection of IONP-HA-GEM-CTX-Cy5.5. Cell nucleus were stained with DAPI (blue); endothelial cells were stained with anti-CD31 antibody (green) and NPs were red (false-coloured). Blood vessels are highlighted in dashed circles. The scale bar corresponds to 100 µm and applies to all photos.

NP localization in various organs was quantified by an IVIS 200 imaging system. To avoid the autofluorescence of tissues, the excitation was set to be 710 nm and the emission was set to be 810–875 nm. The distribution of IONP-HA-GEM-CTX-Cy5.5 in wild type mice is shown in Figure 3b. IONP-HA-GEM-CTX-Cy5.5 had the highest accumulation in the liver at 3 h but was eliminated more than 50% at 48 h. The spleen also showed NP signal at 3 h with a slight increase at 48 h.

The kidney had the second strong signal at 3 h among all organs with moderate decrease at 48 h. Based on these information, it can be expected that IONP-HA-GEM-CTX-Cy5.5 mainly degraded in liver and excreted through renal system. There was nearly no signal from the heart and low signal from the brains. Since these wild type mice had no tumours in the brains, it is expected that no many NPs would accumulate in the brains. However, it is imperative to know whether IONP-HA-GEM-CTX-Cy5.5 is able to cross the BBB in vivo and thus serve as a potential drug delivery carrier for the GBM treatment.

To evaluate BBB permeability of IONP-HA-GEM-CTX-Cy5.5, we analyzed brain sections of mice 2 h and 6 h after intravenous injections of NPs (Figure 4). Tissue sections were stained with anti-CD31 antibody for visualization of endothelial blood vessels and DAPI for nuclei. The brain tissues from untreated mouse showed no signal from NPs (top row). The images from the mouse 2 h after NP administration showed several red dots near blood vessels indicating extravasation of NPs from blood vessels (middle row). There were some NPs around blood vessels at 6 h (bottom row) but the amount were much less than those at 2h. This result and the biodistribution result shown in Figure 3b suggest that IONP-HA-GEM-CTX-Cy5.5 was able to pass the BBB in live mice and accumulate in brains, although only a small amount of NPs were observed, because these mice did not bear brain tumours. A higher NP amount in brains of tumour-bearing mice is expected because of the active targeting mediated by CTX.[23, 26, 34]

Conclusions

IONP-HA-GEM-CTX produced in this study has small size, uniform shape, and great stability in biological medium. Significantly, IONP-HA-GEM-CTX effectively entered and killed GBM cells, had prolonged blood circulation, and was excreted from renal system. Furthermore, the NPs demonstrated the ability to cross the BBB in live mice. Our experimental results suggest that IONP-HA-GEM-CTX has the potential to improve *in vivo* performance of GEM.

Acknowledgements

The work is supported by NIH grant R01CA161953. Q. M. acknowledges support from an NIH Ruth L. Kirschstein T32 Fellowship (T32CA138312). We also acknowledge the support from NIH to UW Keck Microscopy Facility (S10OD016240).

Notes and references

1. S. Hoelder, P. A. Clarke and P. Workman, *Molecular Oncology*, 2012, **6**, 155-176.
2. T. M. Allen and P. R. Cullis, *Science*, 2004, **303**, 1818-1822.
3. R. A. Petros and J. M. DeSimone, *Nat Rev Drug Discov*, 2010, **9**, 615-627.

4. S. Noble and K. L. Goa, *Drugs*, 1997, **54**, 447-472.
5. C. Nabhan, N. Krett, V. Gandhi and S. Rosen, *Current Opinion in Oncology*, 2001, **13**, 514-521.
6. V. Heinemann, *Oncology*, 2001, **60**, 8-18.
7. M. D. Shelley, G. Jones, A. Cleves, T. J. Wilt, M. D. Mason and H. G. Kynaston, *Bju International*, 2012, **109**, 496-505.
8. V. Heinemann, *Oncology*, 2003, **64**, 191-206.
9. D. Lorusso, A. Di Stefano, F. Fanfani and G. Scambia, *Annals of Oncology*, 2006, **17**, v188-v194.
10. B. Geoerger, J. Chisholm, M.-C. Le Deley, J.-C. Gentet, C. M. Zwaan, N. Dias, T. Jaspan, K. Mc Hugh, D. Couanet, S. Hain, A. Devos, R. Riccardi, C. Cesare, J. Boos, D. Frappaz, P. Leblond, I. Aerts and G. Vassal, *European Journal of Cancer*, 2011, **47**, 230-238.
11. M. Morfouace, A. Shelat, M. Jacus, Burgess B. Freeman Iii, D. Turner, S. Robinson, F. Zindy, Y.-D. Wang, D. Finkelstein, O. Ayrault, L. Bihannic, S. Puget, X.-N. Li, James M. Olson, Giles W. Robinson, R. K. Guy, Clinton F. Stewart, A. Gajjar and Martine F. Roussel, *Cancer Cell*, 2014, **25**, 516-529.
12. G. Metro, A. Fabi, M. Mirri, A. Vidiri, A. Pace, M. Carosi, M. Russillo, M. Maschio, D. Giannarelli, D. Pellegrini, A. Pompili, F. Cognetti and C. Carapella, *Cancer Chemotherapy and Pharmacology*, 2010, **65**, 391-397.
13. L. A. Shipley, T. J. Brown, J. D. Cornpropst, M. Hamilton, W. D. Daniels and H. W. Culp, *Drug Metabolism and Disposition*, 1992, **20**, 849-855.
14. B. R. Sloat, M. A. Sandoval, D. Li, W.-G. Chung, D. S. P. Lansakara-P, P. J. Proteau, K. Kiguchi, J. DiGiovanni and Z. Cui, *International Journal of Pharmaceutics*, 2011, **409**, 278-288.
15. J. L. Arias, L. H. Reddy and P. Couvreur, *Langmuir*, 2008, **24**, 7512-7519.
16. S. Rejiba, L. H. Reddy, C. Bigand, C. Parmentier, P. Couvreur and A. Hajri, *Nanomedicine-Nanotechnology Biology and Medicine*, 2011, **7**, 841-849.
17. E. Dalla Pozza, C. Lerda, C. Costanzo, M. Donadelli, I. Dando, E. Zoratti, M. T. Scupoli, S. Beghelli, A. Scarpa, E. Fattal, S. Arpicco and M. Palmieri, *Biochimica Et Biophysica Acta-Biomembranes*, 2013, **1828**, 1396-1404.
18. G. Arya, M. Vandana, S. Acharya and S. K. Sahoo, *Nanomedicine-Nanotechnology Biology and Medicine*, 2011, **7**, 859-870.
19. C.-X. Wang, L.-S. Huang, L.-B. Hou, L. Jiang, Z.-T. Yan, Y.-L. Wang and Z.-L. Chen, *Brain Research*, 2009, **1261**, 91-99.
20. P. Y. Wen and S. Kesari, *New England Journal of Medicine*, 2008, **359**, 492-507.
21. C. Fang, N. Bhattarai, C. Sun and M. Q. Zhang, *Small*, 2009, **5**, 1637-1641.
22. C. Sun, J. S. H. Lee and M. Zhang, *Advanced Drug Delivery Reviews*, 2008, **60**, 1252-1265.
23. Z. R. Stephen, F. M. Kievit, O. Veiseh, P. A. Chiarelli, C. Fang, K. Wang, S. J. Hatzinger, R. G. Ellenbogen, J. R. Silber and M. Zhang, *ACS Nano*, 2014, **8**, 10383-10395.
24. N. Kohler, G. E. Fryxell and M. Zhang, *Journal of the American Chemical Society*, 2004, **126**, 7206-7211.
25. J. Deshane, C. C. Garner and H. Sontheimer, *Journal of Biological Chemistry*, 2003, **278**, 4135-4144.
26. O. Veiseh, C. Sun, C. Fang, N. Bhattarai, J. Gunn, F. Kievit, K. Du, B. Pullar, D. Lee, R. G. Ellenbogen, J. Olson and M. Zhang, *Cancer Research*, 2009, **69**, 6200-6207.
27. C. Fang, O. Veiseh, F. Kievit, N. Bhattarai, F. Wang, Z. Stephen, C. Li, D. Lee, R. G. Ellenbogen and M. Zhang, *Nanomedicine*, 2010, **5**, 1357-1369.
28. L. Brannon-Peppas and J. O. Blanchette, *Advanced Drug Delivery Reviews*, 2012, **64, Supplement**, 206-212.
29. G. D. Prestwich, D. M. Marecak, J. F. Marecek, K. P. Vercruysse and M. R. Ziebell, *Journal of Controlled Release*, 1998, **53**, 93-103.
30. M. M. Yallapu, N. Chauhan, S. F. Othman, V. Khalilzad-Sharghi, M. C. Ebeling, S. Khan, M. Jaggi and S. C. Chauhan, *Biomaterials*, 2015, **46**, 1-12.
31. M. S. Bobola, S. Varadarajan, N. W. Smith, R. D. Goff, D. D. Kolstoe, A. Blank, B. Gold and J. R. Silber, *Clinical Cancer Research*, 2007, **13**, 612-620.
32. N. Gaspar, L. Marshall, L. Perryman, D. A. Bax, S. E. Little, M. Viana-Pereira, S. Y. Sharp, G. Vassal, A. D. J. Pearson, R. M. Reis, D. Hargrave, P. Workman and C. Jones, *Cancer Research*, 2010, **70**, 9243-9252.
33. C. Fang, F. M. Kievit, Y. C. Cho, H. Mok, O. W. Press and M. Zhang, *Nanoscale*, 2012, **4**, 7012-7020.
34. F. M. Kievit, O. Veiseh, C. Fang, N. Bhattarai, D. Lee, R. G. Ellenbogen and M. Q. Zhang, *Acs Nano*, 2010, **4**, 4587-4594.

Graphic TOC

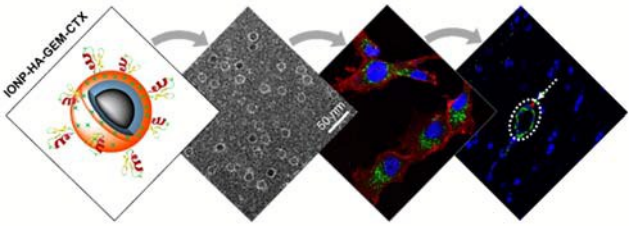

A nanoparticle bearing gemcitabine and chlorotoxin shows efficient cancer cell uptake and killing, extended blood half-life, and blood-brain barrier penetration.

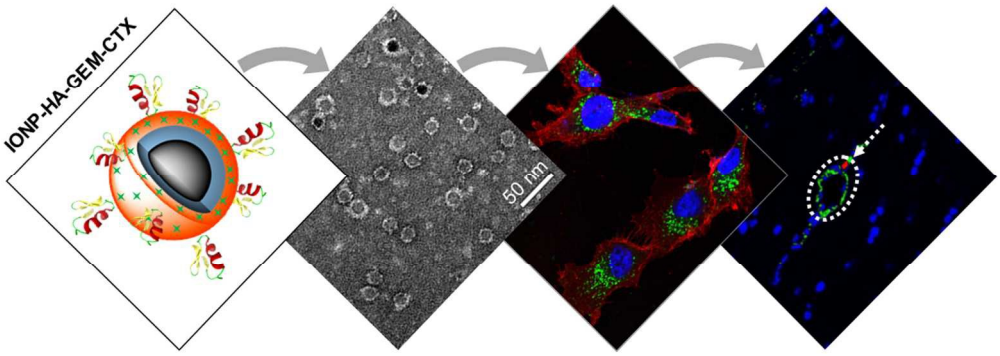

203x72mm (300 x 300 DPI)